



## Article

# Case Study of Contaminant Transport Using Lagrangian Particle Tracking Model in a Macro-Tidal Estuary

Bon-Ho Gu <sup>1</sup>, Seung-Buhm Woo <sup>2</sup>, Jae-Il Kwon <sup>1</sup>, Sung-Hwan Park <sup>1</sup> and Nam-Hoon Kim <sup>1,\*</sup>

<sup>1</sup> Coastal Disaster & Safety Research Department, Sea Power Enhancement Research Division, Korea Institute of Ocean Science & Technology, Busan 49111, Republic of Korea; bhgu@kiost.ac.kr (B.-H.G.); jikwon@kiost.ac.kr (J.-I.K.); spark@kiost.ac.kr (S.-H.P.)

<sup>2</sup> Department of Ocean Science, Inha University, Incheon 22212, Republic of Korea; sbwoo@inha.ac.kr

\* Correspondence: nhkim0426@kiost.ac.kr; Tel.: +82-51-664-3708

**Abstract:** This study presents a comprehensive analysis of contaminant transport in estuarine environments, focusing on the impact of tidal creeks and flats. The research employs advanced hydrodynamic models with irregular grid systems and conducts a detailed residual current analysis to explore how these physical features influence the movement and dispersion of contaminants. The methodology involves simulating residual currents and Lagrangian particle trajectories in both ‘Creek’ and ‘No Creek’ cases, under varying tidal conditions. The results indicate that tidal creeks significantly affect particle retention and transport, with notable differences observed in the dispersion patterns between the two scenarios. The ‘Creek’ case demonstrates enhanced material retention along the creek pathways, while the ‘No Creek’ case shows broader dispersion, potentially leading to increased sedimentation in open sea areas. The discussion highlights the implications of these findings for sediment dynamics, contaminant transport, and estuarine ecology, emphasizing the role of tidal creeks in modulating flow and material transport. The research underlines the necessity of incorporating detailed environmental features in estuarine models for accurate contaminant transport prediction and effective estuarine management. This study contributes to a deeper understanding of estuarine hydrodynamics and offers valuable insights for environmental policy and management in coastal regions.



**Citation:** Gu, B.-H.; Woo, S.-B.; Kwon, J.-I.; Park, S.-H.; Kim, N.-H. Case Study of Contaminant Transport Using Lagrangian Particle Tracking Model in a Macro-Tidal Estuary. *Water* **2024**, *16*, 617. <https://doi.org/10.3390/w16040617>

Academic Editor: Constantinos V. Chrysikopoulos

Received: 25 January 2024

Revised: 8 February 2024

Accepted: 18 February 2024

Published: 19 February 2024



**Copyright:** © 2024 by the authors. Licensee MDPI, Basel, Switzerland. This article is an open access article distributed under the terms and conditions of the Creative Commons Attribution (CC BY) license (<https://creativecommons.org/licenses/by/4.0/>).

**Keywords:** macro-tidal estuary; unstructured grid model; residual volume transport; Lagrangian particle tracking; Stokes drift; contaminant transport

## 1. Introduction

Tidal waves from the open ocean undergo various transformations as they enter estuaries and are influenced by various factors, such as freshwater inputs, water depth, and topography [1–5]. These transformations create asymmetry in tidal curves, leading to significant differences in sediment transport during flood and ebb tides. This variation affects the overall estuarine hydrodynamic system, making an understanding of the flood and ebb dominance phenomenon crucial in regions where tides are a significant driving force. Historically, estuarine areas have undergone development for various coastal projects, such as dyke construction, airport development, and bridge construction. More recently, they have become key sites for offshore wind and tidal current power generation. These developments alter the adjacent coastal topography and water flow characteristics, necessitating predictions of marine environmental changes due to the ongoing coastal development pressures. To assess and predict these impacts and establish conservation strategies, various numerical models have been employed. In [6], the authors explored spatiotemporal changes and annual variability in residual currents through long-term fixed-point observations, indicating that freshwater flux affects residual current characteristics. In [7], the authors observed that tidal propagation characteristics in coastal waters vary

spatially in amplitude due to bottom friction and topographic convergence near narrow tidal straits. Furthermore, [8] estimated material transport amounts during neap and spring tides using the two-dimensional POM (Princeton Ocean Model).

The research focusing on the numerical simulation of intertidal zones has made notable contributions. In [9], the authors employed MIKE21 to analyze the impact of intertidal simulation on numerical model results in domestic waters. This study identified that the inclusion of the intertidal zone significantly affects overall seawater flow in the models. Further extending this research, [9] applied three different hydrodynamic models in Gomso Bay, Korea—EFDC (Environmental Fluid Dynamics Code), ESCORT (Efficient Support for Coastal Ocean Research and Test), and MIKE21; each of these models involved the employment of distinctly different methods and intertidal simulation techniques. This research entailed a comparative analysis of the intertidal simulation characteristics of each model and provided insights into their respective efficiencies and accuracies in simulating intertidal zones. Despite the advances, the existing research often inadequately represents the complex coastal features and dynamic interactions between environmental factors. Most models face challenges in accurately simulating intricate processes like sediment transport, contaminant dispersion, and ecological responses in estuarine environments. Additionally, the computational demand and extensive data required for model calibration and validation pose challenges, especially in modeling dynamic estuarine systems with significant spatial and temporal variability.

To address the limitations identified in previous studies and to accurately predict the circulation of contaminants, particularly in environments characterized by significant tidal range variations, our research adopts a novel approach focusing on residual currents. This distinctive aspect of our study addresses the need for more precise modeling in estuarine environments where the interplay of tides, topography, and hydrodynamic forces plays a crucial role in influencing the transport and fate of pollutants. The inclusion of residual currents in our analysis facilitates a more nuanced understanding of material transport within estuarine systems. Often overlooked or overly simplified in the traditional modeling approach, residual currents play a crucial role in the long-term movement of water and associated materials, including contaminants. Our approach accounts for the complexities of these currents, particularly in the context of estuarine environments, encompassing the influences of both tidal creeks and flat areas. Furthermore, the use of irregular grids enables a more accurate representation of the intricate coastal and tidal channel topographies, which are essential in understanding the patterns of contaminant dispersion and accumulation. This methodological advancement provides a finer resolution in areas of interest, ensuring that even the small-scale but significant topographical features influencing flow dynamics are adequately captured.

The primary objective of this research is to comprehensively analyze and understand the dynamics of contaminant transport in estuarine environments, with a specific focus on the role of tidal creeks and flats. By employing advanced hydrodynamic models that integrate both irregular grid systems and detailed residual currents analyses, this study aims to provide a more accurate and nuanced understanding of how contaminants move and disperse in complex estuarine systems. To achieve this objective, the paper is organized into the following sections: After Section 1, the introduction, the methodology is detailed, encompassing the employed hydrodynamic model, the simulation setup, and the specific parameters for residual currents and particle tracking. The Section 3 then offers a comprehensive examination of residual currents and particle movements in both 'Creek' and 'No Creek' scenarios under varying tidal conditions. Following this, the Section 4 interprets these findings and considers their implications for estuarine sediment dynamics, contaminant transport, and the overall ecological health of these environments. This section further explores the wider relevance of the study's outcomes in the context of estuarine management and conservation. Then, the paper concludes with a summary of the principal findings, emphasizing the importance of incorporating detailed environmental features and residual currents in estuarine models for the precise prediction and effective management

of contaminant transport. The conclusion highlights the contribution of our research to a broader understanding of estuarine dynamics and the advancement of sustainable environmental strategies.

## 2. Materials and Methods

### 2.1. Study Area

Gyeonggi Bay (GGB), located in the Yellow Sea of Korea (Figure 1), is a macro-tidal flat with a complex coastline and a tidal range exceeding 8 m. GGB is affected by major freshwater inputs from the Han, Imjin, and Yesong rivers, with the influx of freshwater being particularly concentrated during the summer (June to August). Although there are seasonal variations in GGB, where the freshwater influence is strong, it is more appropriate to analyze the currents that include the effects of freshwater, rather than solely considering tidal dominance in the ebb and flood tides. The bay has undergone various coastal development projects, such as the construction of the Sihwa Tidal Power Plant and the Incheon New Harbor project. These coastal developments have led to significant alterations in the estuarine circulation; they particularly impacted the flow characteristics near Sihwa Lake prior to the operation of the Sihwa Tidal Power Plant in 2012. Understanding these changes in estuarine circulation is crucial for predicting the paths of the pollutants and sediments resulting from coastal developments.

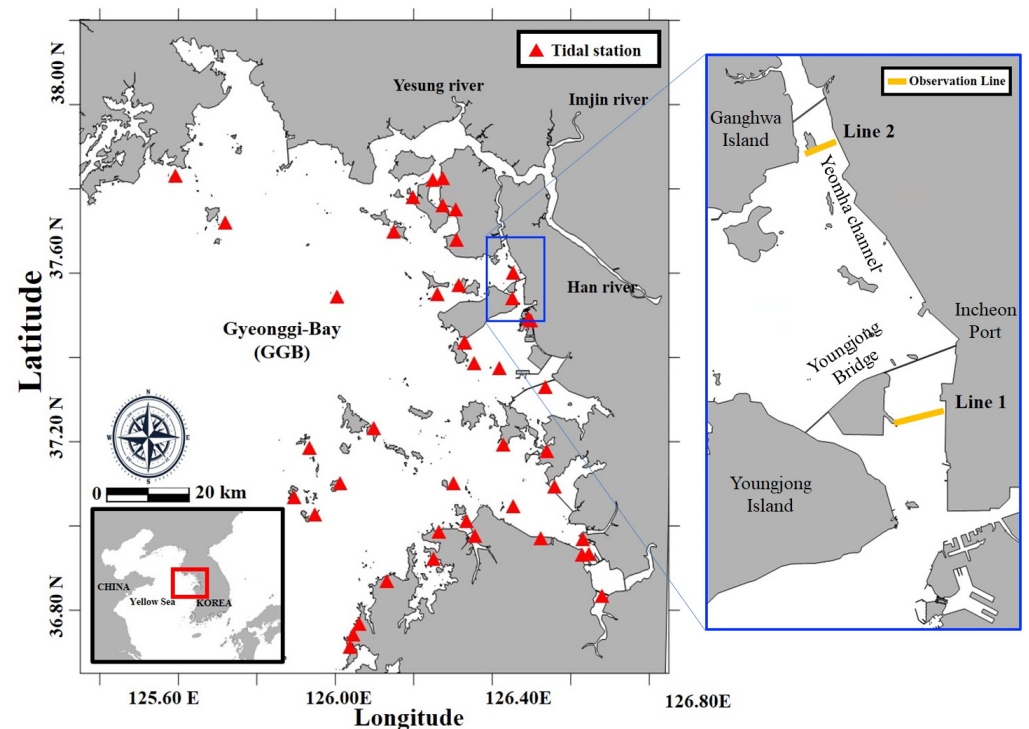


**Figure 1.** Map of Gyeonggi Bay (GGB) with observation sites. The red triangles represent tidal stations operated by the Korea Hydrographic and Oceanographic Agency (KHOA), utilized for model validation. The yellow lines in the blue box indicate Acoustic Doppler Current Profiler (ADCP) shipborne measurements.

### 2.2. Numerical Model

The Finite Volume Coastal Ocean Model (FVCOM), used in this study, is a three-dimensional numerical model developed by [10]. It is specifically designed to accurately simulate flow and material transport in coastal and estuarine regions; accurate simulation is essential for representing intertidal zones, tidal channels, and wetlands. The model employs a three-dimensional mass conservation technique with a wet/dry treatment to adeptly handle these complex areas. Additionally, to precisely replicate irregular topogra-

phy, the FVCOM uses a sigma coordinate system vertically and non-orthogonal triangular grids horizontally. Bottom friction is calculated using a quadratic formula based on the friction coefficient at the boundary layer between the sediment and water layers. For horizontal eddy viscosity, the Smagorinsky diffusion coefficient is utilized, and the turbulence diffusion model adopts the Mellor–Yamada level 2.5 turbulent closure scheme. A detailed description of the model can be found in [10].

The intertidal treatment technique employed in the FVCOM categorizes a water layer as an exposed intertidal zone (drying) when its thickness is less than a critical value and as a submerged area (wetting) when the thickness exceeds this threshold. This approach is particularly effective in coastal areas with complex coastlines, where the distinction between land and ocean is challenging. The unstructured grid system effectively handles this intertidal treatment. When a triangular cell is treated as dry, its velocity is set to zero, and it is subsequently excluded from the Tracer Control Element (TCE) flux calculations. This technique ensures accurate mass conservation within the TCE that encompasses the dynamic boundary between wet and dry cells; in this manner, it allows the calculation of both the TCE flux and the Momentum Control Element (MCE) flux.

The FVCOM includes a Lagrangian particle tracking (LPT) module, which involves solving a nonlinear system of ordinary differential equations to simulate the movement of particles within the model domain. This module allows the incorporation of a random walk-type process to address subgrid-scale turbulent variability in the velocity field; this is a common approach used by many practitioners to enhance model realism. The LPT module in the FVCOM offers a sophisticated method to trace the paths of neutral particles across the model domain, utilizing the 3-D velocity field. To initiate the tracking, initial particle locations are specified in a dedicated data file. During model execution, the particle location and velocity data are recorded at predetermined intervals, with the results stored in the out subdirectory of the designated output directory, as indicated by the output files. The model time, as well as the true Cartesian coordinates for each particle, is documented. In cases where the particles traverse beyond the horizontal bounds of the domain, they are retained at their last known position with zero velocity, and the elnum in the log file is assigned the value of zero.

### 2.3. Field Measurements

In this study, we utilized the Acoustic Doppler Current Profiler (ADCP) observational data, as presented in [11], to understand pollutant dispersion in coastal environments. The shipborne measurements utilized a 600 kHz ADCP (Teledyne RD Instruments Co., Ltd., San Diego, CA, USA), which was mounted to the side of the vessel, enabling the efficient acquisition of multi-layer velocity and directional data, along with cross-sectional velocity data. The device was positioned 0.8 m below the sea surface, and the bin size was set to 1 m to obtain multi-layer velocity and direction. The ADCP measurements were conducted over 13 h periods during spring and neap tides at two transects downstream of the channel and at the mid-point of the channel, as shown in Figure 1. Transect Line 1, with an average depth of about 10 m and a channel width of approximately 1600 m, is located near the Incheon port. It narrows sharply from the open sea, exhibiting a depth of about 13 m on the east side and 12 m on the west side. The west side characterizes a gently sloping intertidal zone, while the east side exhibits a steep decline in depth towards the land. Transect Line 2, situated between Yeongjong Island and Ganghwa Island, features shallow waters with an average depth of about 6 m and is influenced by seawater inflow from the wide tidal flats and by the high concentrations of suspended sediments. The data collection for Line 1 and Line 2 during neap tide was carried out in June 2009, while for spring tide, it was conducted in October 2010 for Line 1 and June 2009 for Line 2. Post-processing of the observed velocity data was conducted as described in [11], including ensemble averaging, outlier removal, angle correction, and transformation to horizontal and vertical sigma coordinate systems. The final processed data served as the representative cross-sectional current velocity for our research [11].

#### 2.4. Experiment Design

For the primary objective of this study, which is to understand the circulation of contaminant transport due to tidal channels, experiments were configured based on the grid structures of the 'Creek' and 'No Creek' cases (Figure 2). The bathymetry was taken from KHOA's digital chart, and the horizontal resolution was set to about 20–300 m at the mouth of the Han River, with the resolutions in other areas dynamically adjusted to enhance computational resource efficiency. As shown in Figure 2, the 'No Creek' case replicated the tidal creek at the southern end of Ganghwa Island, with an average resolution of about 100 m. In contrast, the 'Creek' case grid, which was designed to better represent rapidly changing depths, processed the tidal creek's resolution at a higher level than the surrounding grids to more accurately simulate material transport within the tidal creek. Both experiments were adjusted to have a similar number of total grids, with the grid distributions outside the intertidal zone and tidal channels precisely matched. Despite having a similar number of nodes, the 'Creek' case was set to show a spatial resolution of about 20 m in areas with steep depth gradients, such as tidal creeks, while in areas with gentle depth gradients, such as tidal flats, the resolution was set to a maximum of 300 m. All the parameters necessary for the simulation, including bottom roughness and open boundary conditions, were identical in both experiments; thus, any differences are attributable to whether the tidal creek was considered. By comparing the two experiments, it is possible to understand the impact of resolution adjustment due to the tidal creek on residual transport and the contamination spread in a macro-tidal flat environment.

The open boundary conditions shared by both experiments were constructed by linearly interpolating the harmonic constants of the main four tidal constituents ( $M_2$ ,  $S_2$ ,  $K_1$ ,  $O_1$ ) using results from the TOPEX/POSEIDON-based tide model NAO99.Jb. Freshwater conditions were input using daily flow rates from the Water Resource Management Information System (WAMIS), and the locations where freshwater inflows were indicated are shown in Figure 1. The freshwater inflow from the Han River was calculated using the residual volume transport data observed at the southern end of Yeomha Channel and near Youngjong Bridge during flood and slack tides in June 2009 and the discharge data provided by WAMIS from June to July 2009 from the Paldang DAM, which is located in the upstream of the Han River. The freshwater inflow from the Yesung River was determined by calculating the inflow area ratio from the Han River, and the inflow from the Imjin River was calculated using the flow rates from Gunnam/Jeongok, which is the monitoring station of the water level.

The initial water level of the model was set to Mean Sea Level (MSL), and the initial temperature and salinity were uniformly set across all layers at constant values (15 °C, 30 psu), assuming homogeneity throughout the ocean, followed by a one-year spin-up. The external time step was set to 0.5 s to satisfy the Courant–Friedrichs–Lewy (CFL) condition, and the internal time step was set to 5 s. The vertical layer was set to 11 layers to maintain consistent vertical resolution even in shallow intertidal zones. The wet/dry minimum depth was set to 0.05 m, which was slightly less than the limit value of 0.07 m suggested by [9], to ensure model stability and accuracy. The total simulation period was set to 40 days to ensure that the four major tidal constituents input into the open boundary condition could be sufficiently decomposed.

For tidal calibration and validation of the model, hourly tide data from 42 tide stations operated by the KHOA across the Gyeonggi Bay area were collected. The collected harmonic constants were decomposed using the analysis tool developed by [12] and then used for tidal validation. In addition, the LPT module was employed to place virtual particles around the tidal flat in both models, tracking their trajectories during the simulation period. The particle movement trajectories in the 'Creek' and 'No Creek' cases were compared during spring and neap tides. The particles were exposed for a 40-day simulation period to observe their long-term trajectories. The average movement trajectories of the particles were also compared based on the two experiments to confirm whether the tidal creek influences the transport mechanism of the pollutants.

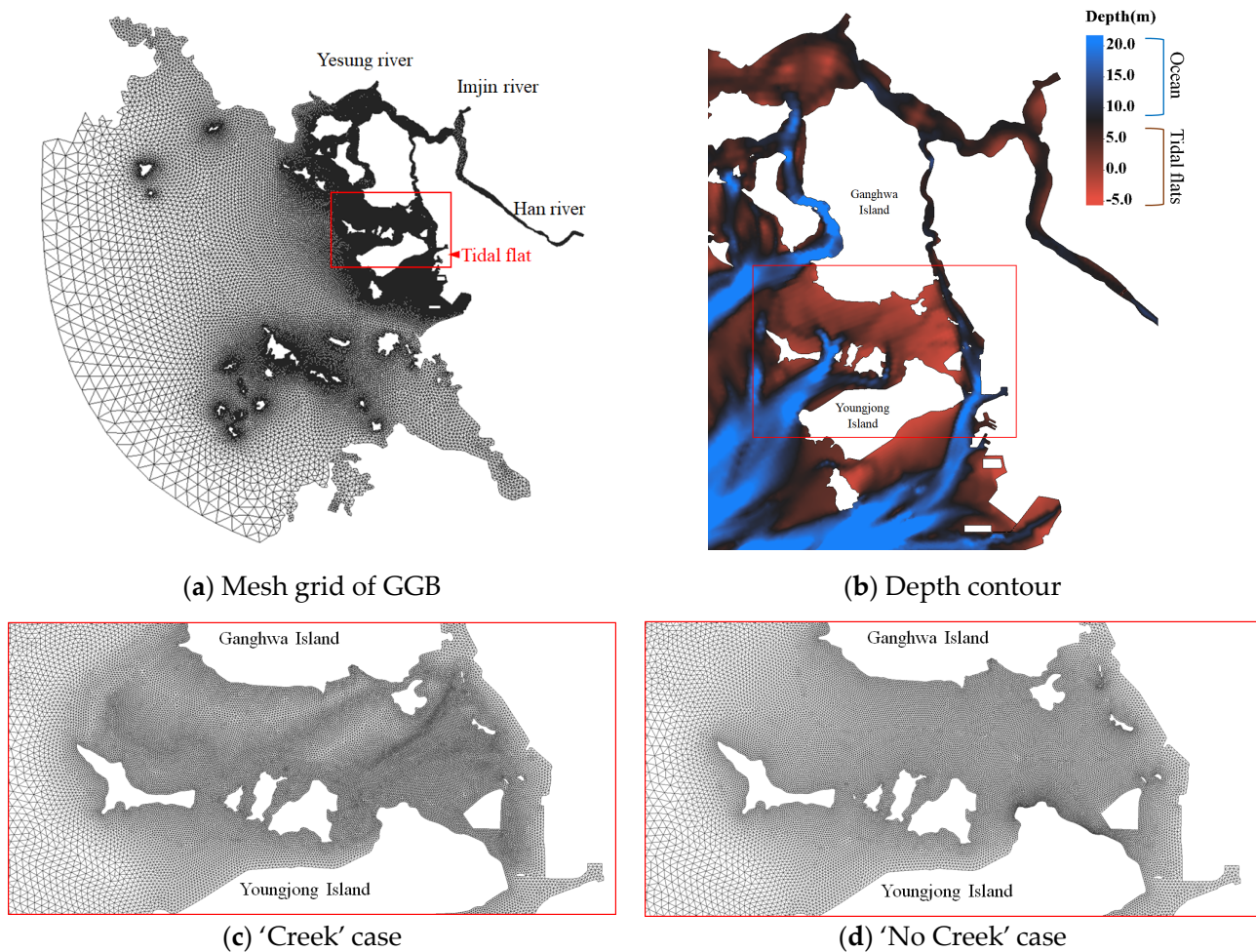


**Figure 2.** (a) The unstructured mesh grid of Gyeonggi Bay (GGB) includes the tidal flat marked with a red box. (b) The depth contour focuses on the tidal flats. The model domain for this study is divided into two scenarios: (c) Creek and (d) No Creek cases. The 'Creek' case incorporates the tidal channel between Ganghwa Island and Yeongjong Island, representing the rapidly changing depths with high resolution. The 'No Creek' case, on the other hand, grids the intertidal zone areas with uniform high resolution, without considering the tidal channel.

### 3. Results

#### 3.1. Model Validation

In Figure 3, the 'Creek' and 'No Creek' cases exhibit distinct correlations with the observational data (OBS) for the four main tidal constituents ( $M_2$ ,  $S_2$ ,  $K_1$ ,  $O_1$ ). The 'Creek' case shows a strong alignment with the OBS, as evidenced by an average correlation coefficient exceeding 0.95. This high correlation highlights a significant congruence in the amplitude and phase measurements, which is especially pronounced for the  $M_2$  and  $O_1$  constituents. For these constituents, the amplitudes closely follow the 1:1 line up to about 350 cm for  $M_2$  and 150 cm for  $O_1$ , with phase angles indicating tight concordance. On the other hand, the 'No Creek' case presents a slightly lower, yet still noteworthy, average correlation coefficient of 0.91. Despite this minor divergence, particularly in the  $S_2$  and  $K_1$  constituents, with maximum amplitudes around 250 cm for  $S_2$  and 100 cm for  $K_1$ , the results remain robust. The phase data for the 'No Creek' case show a modest deviation from the ideal 1:1 correspondence, with  $S_2$  exhibiting the largest discrepancy. Nonetheless, the tidal predictions for both cases are considered reliable, given that the correlation coefficients for both exceed 0.90.

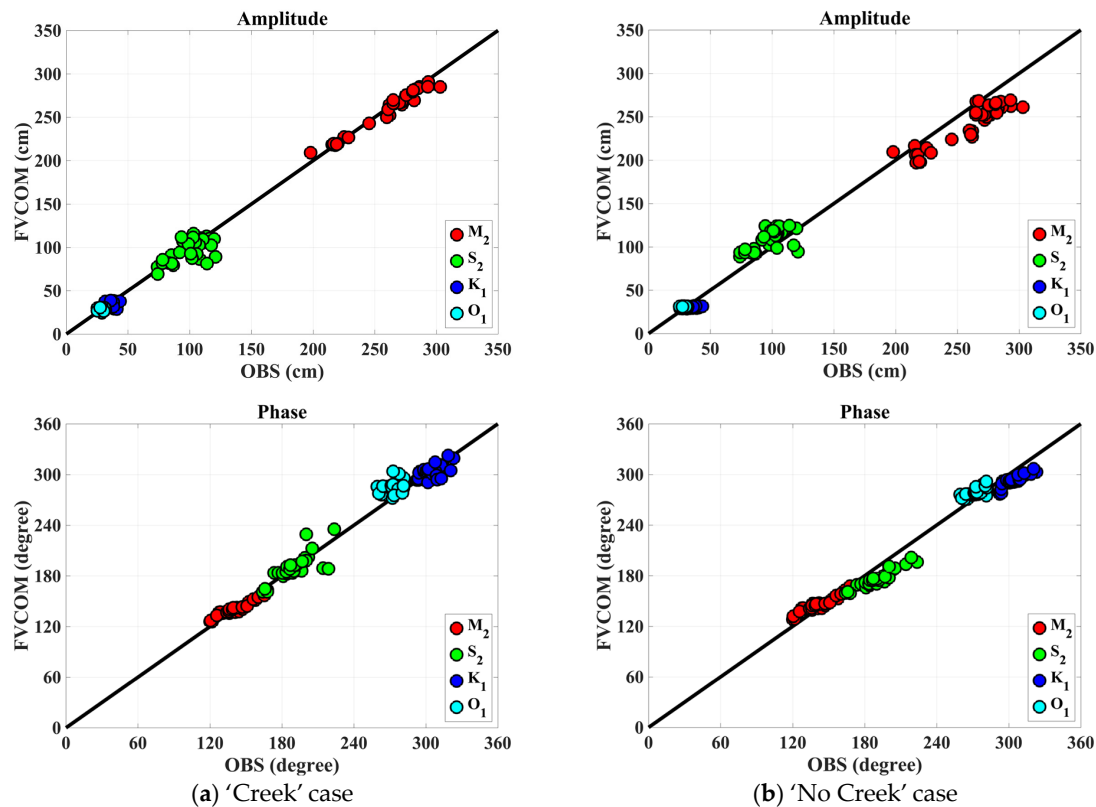


**Figure 3.** The 1:1 correlation plots of the ‘Creek’ and ‘No Creek’ cases against observational data (OBS) for the four major tidal constituents ( $M_2$ ,  $S_2$ ,  $K_1$ ,  $O_1$ ). (a) The ‘Creek’ case with amplitudes and phases closely clustered around the 1:1 line, indicating a high level of agreement between the model result (FVCOM) and OBS, particularly for  $M_2$  and  $O_1$  constituents. (b) The ‘No Creek’ case, which shows a slightly wider distribution of data points but still maintains a substantial alignment with the OBS, indicating reliable model predictions. Both panels collectively highlight the model’s adeptness at capturing tidal dynamics.

### 3.2. Residual Volume Transport

Figure 4 provides an insightful comparison of the residual currents between the ‘Creek’ and ‘No Creek’ cases during both the spring and neap tides; the comparison employs the residual volume transport framework proposed by [13]. For reference, the results of verifying the residual current required to calculate the residual volume transport are summarized in Appendix A (Figure A1). A notable aspect of this study is the significant surface residual current, of approximately 0.15 m/s, located south of the tidal channel, which attenuates with depth. The influence of this surface residual current is observed to extend into the subsurface layers, becoming almost negligible at the bottom layer despite the diminishing intensity. Upon analyzing the ‘Creek’ and ‘No Creek’ cases, it is evident that differences in the residual currents are more distinct in the Stokes drift compared to the Eulerian residuals, particularly in the tidal flats. During both the spring and neap tides, the Stokes drift in the tidal flats exhibits a variation of about 0.1 to 0.2 m/s. This variation tends to amplify with an increasing tidal range, indicating that the Stokes drift significantly influences the residual current differences in these areas. The spatial resolution discrepancy between the tidal creek and the tidal flat, particularly along the depth gradient, highlights a nonlinear difference that is probably inducing variations in the material transport. This effect is particularly pronounced in the macro-tidal flats, where the nonlinearity is relatively magnified during spring tides due to intensified barotropic conditions. Compared to the neap tides, these differences highlight the importance of considering the intertidal slope to improve the predictive accuracy of coastal estuarine models in tide-dominated environments.

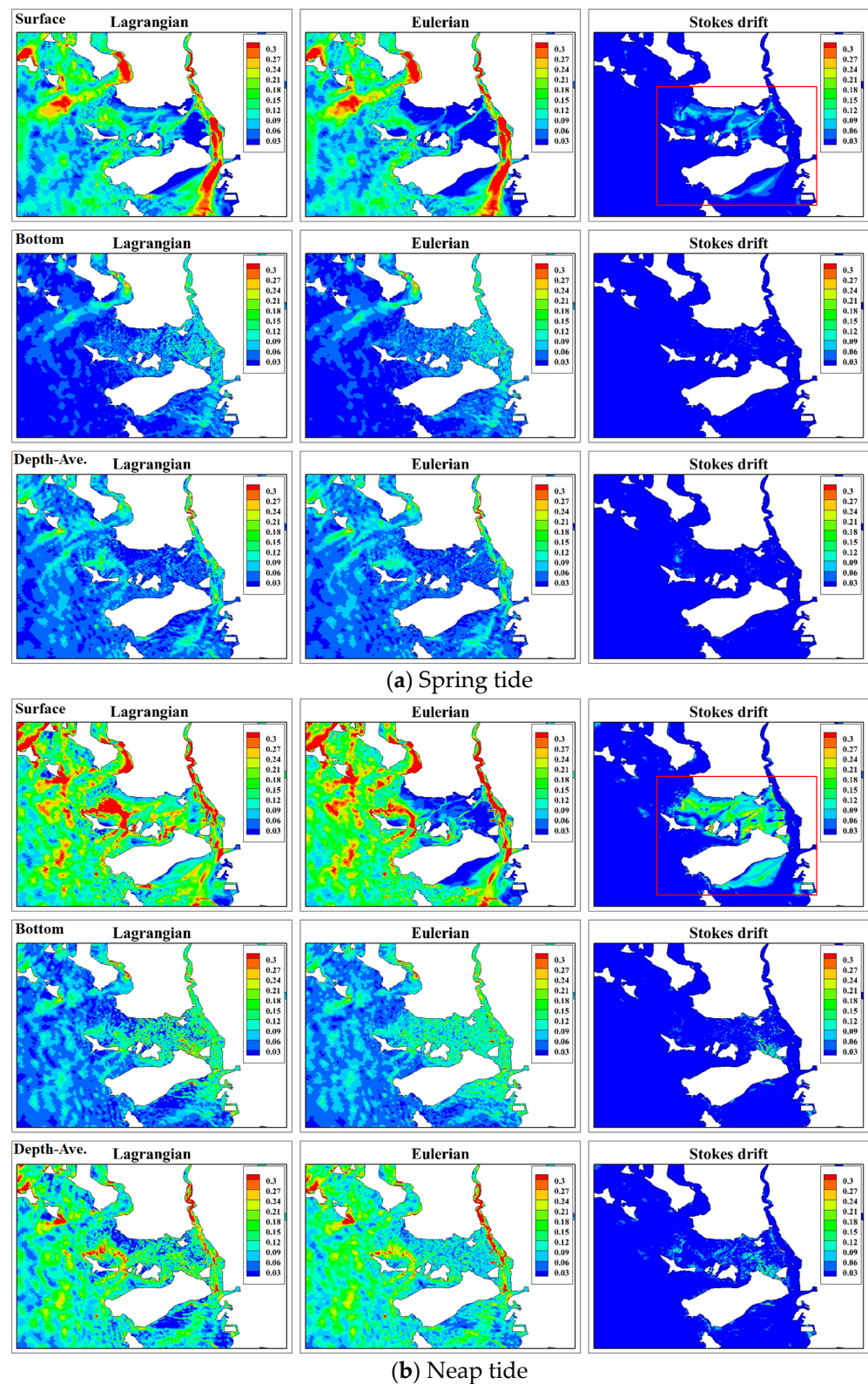


**Figure 4.** Spatial distribution of residual current differences between the ‘Creek’ and ‘No Creek’ cases during (a) spring tide (15–16 June 2009) and (b) neap tide (8–9 June 2009). Each row represents a different vertical layer (surface, bottom, and depth-averaged), and each column corresponds to a different method of residual current calculation (Lagrangian, Eulerian, and Stokes drift) applied between Ganghwa Island and Yeongjong Island. The red boxes indicate the tidal flats. The contour color gradients indicate the velocity magnitude of the residual currents difference (m/s).



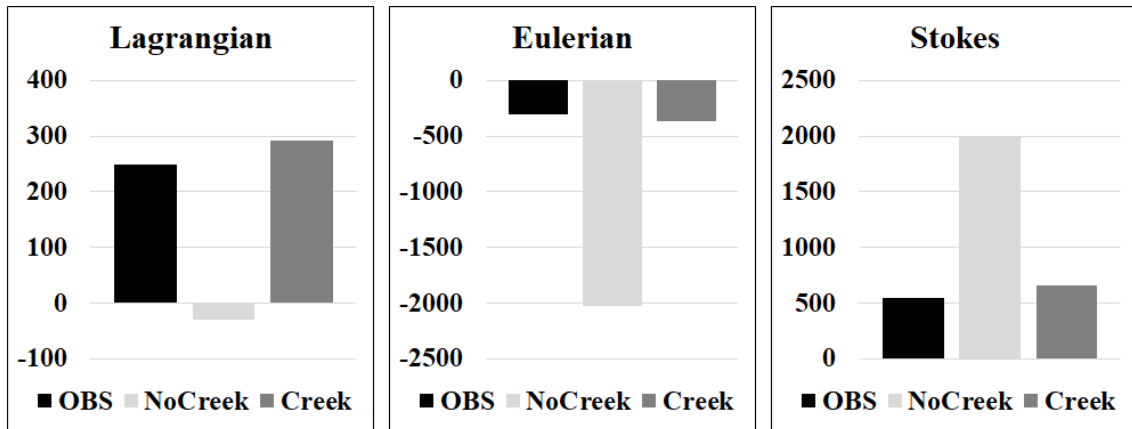
The comprehensive analysis presented in Figure 4 delves into the differences in the residual volume transport between the ‘Creek’ and ‘No Creek’ cases during both spring and neap tides, across the surface and bottom layers and within the depth-averaged residuals. Employing the methodology proposed by [13], our study highlights the intricate differences, particularly in the Stokes drift component, revealing significant variations in the surface layer between Ganghwa Island and Yeongjong Island. These variations underscore the pronounced impact of the tidal flats and channels on the residual transport patterns within the estuary, emphasizing the critical role of geomorphological features in shaping estuarine hydrodynamics. This nuanced examination within the results section of our study elucidates the complex interplay of residual currents, accentuating the necessity of incorporating tidal influences in hydrodynamic models for a precise representation of material transport in estuarine environments.

Figure 5 provides a quantitative evaluation of the residual volume transport across two transects, Line 1 (neap) and Line 2 (neap and spring), based on the ADCP data derived by [11] and calculated using the method described by [13]. For Line 1 during the neap tide, the ‘Creek’ case exhibits a residual volume transport comparable to the OBS across all three methodologies—Lagrangian, Eulerian, and Stokes drift, indicating a well-represented simulation in this specific scenario. In contrast, Line 2 shows an overestimation in both the Eulerian and Stokes drift components compared to the OBS, suggesting discrepancies in these methods or the presence of additional dynamics not fully captured by the model. During the spring tide, the deviation in Line 2 becomes more pronounced, with the Eulerian and Stokes residuals significantly exceeding the OBS. This could indicate a stronger influence of the creek dynamics that are absent in the ‘No Creek’ case. The Lagrangian residual, however, aligns more closely with the observed values, suggesting that it is less sensitive to the complexities introduced by the presence or absence of creeks. The analysis reveals that the ‘Creek’ case generally results in a greater magnitude of residuals, particularly for the Stokes drift, which is several-fold higher in the ‘Creek’ case compared to the ‘No Creek’ case. This pattern persists across both the spring and neap tides, with the spring tide showing a more significant difference, reflecting the impact of stronger tidal forces. For Line 2, the solid downstream gradient from the upper estuarine saltwater leads to the residual volume transport being directed southward (negative values), which contrasts with the dynamics observed in Line 1. Here, in addition to the downstream gradient from the upper estuarine saltwater, Line 1 experiences a significant influence from the strong Stokes drift effect from the western tidal flats, resulting in the final Lagrangian residual volume transport differing from Line 2 by being directed northward. This distinct directional divergence between the two lines underscores the complex interplay of estuarine and tidal flat dynamics in shaping residual transport, highlighting the necessity of considering both upstream saltwater gradients and localized Stokes drift effects to capture the nuanced hydrodynamic behavior within estuarine systems accurately.

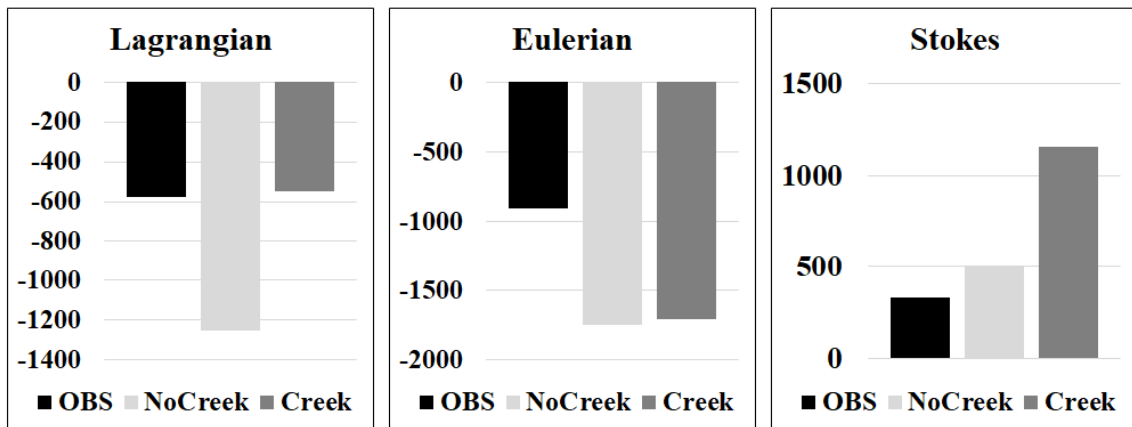
The flow characteristics, under both ebb and flood conditions, show distinct patterns in the residuals. Across both transects, the ‘Creek’ case tends to align more closely with the ebb flow, as indicated by the positive Stokes residuals. This alignment emphasizes the role of the creek in enhancing the seaward transport of materials. This effect is particularly significant during spring tides, when the tidal range and currents reach their peak.

Figure 6 presents a spatial analysis of salinity stratification differences between the surface and bottom layers within the ‘Creek’ and ‘No Creek’ cases, categorized by spring and neap tidal conditions. In the figure, the darker shades indicate areas of enhanced stratification. Notably, the ‘Creek’ case exhibits more pronounced stratification effects, indicating that the inclusion of tidal creeks leads to increased stratification due to the differential residual currents and the associated material transport and mixing processes. During neap tides, the stratification differences are more distinct, implying that the weaker tidal mixing during these periods allows a stronger stratification to persist. This difference is attributable to the variations in residual currents, which influence material transport, thereby affecting stratification and ultimately the overall material circulation within the estuary. Therefore,

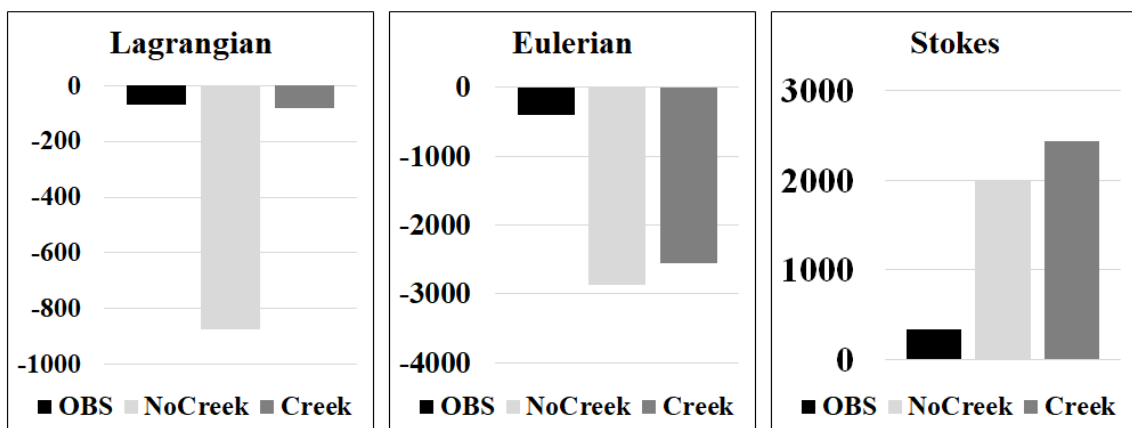
the figure highlights the importance of creek representation in estuarine models, where tidal creeks significantly contribute to the salinity structure and the stratification dynamics over time and space.



(a) Line 1. Neap tide



(b) Line 2. Spring tide



(c) Line 2. Neap tide

**Figure 5.** Comparison of residual volume transport in the ‘Creek’ and ‘No Creek’ cases, calculated based on ADCP data from [11] using the method of [13]. The bar charts represent the residual volume transport ( $m^3/s$ ) across two transects (Line 1 and Line 2) during neap and spring tides. Each panel shows the results derived from the Lagrangian, Eulerian, and Stokes drift.

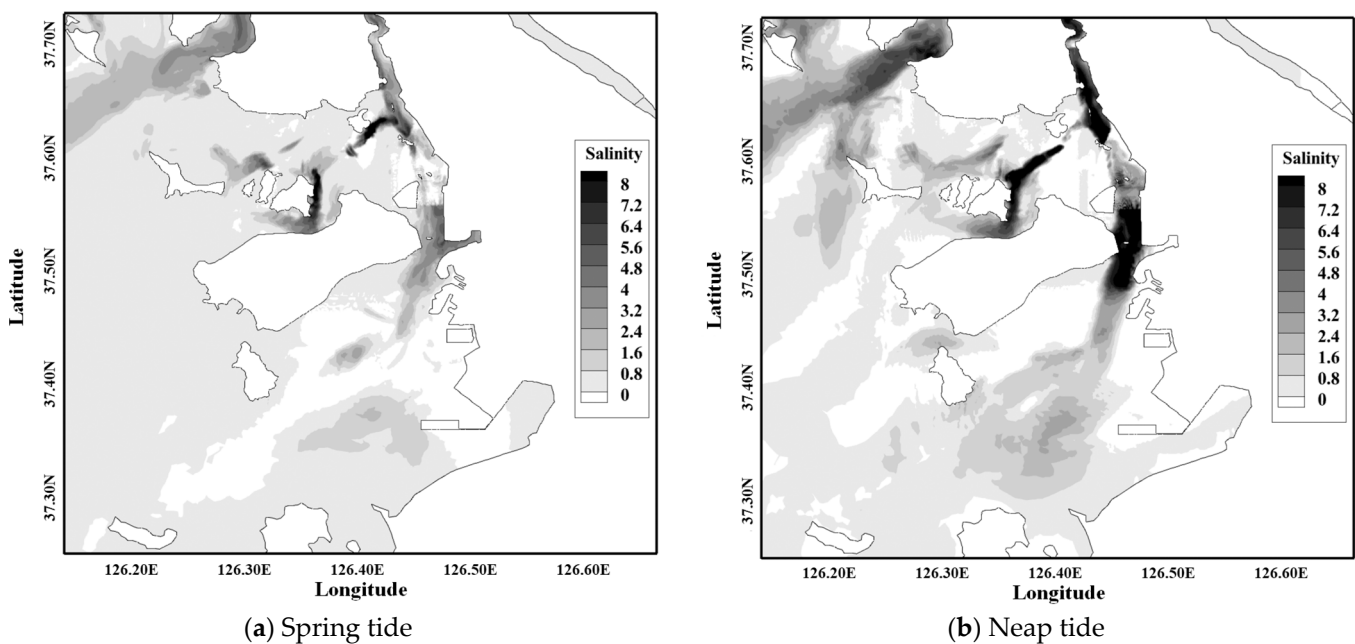


**Figure 6.** Variation in salinity stratification (unit: psu) across the surface and bottom layers during (a) spring tide and (b) neap tide for the ‘Creek’ and ‘No Creek’ cases. Darker shading areas indicate stronger stratification, which is particularly evident during neap tides, suggesting significant spatial–temporal stratification effects due to tidal creek inclusion in the ‘Creek’ case. This highlights the role of tidal creek-induced residuals in altering material transport and estuarine circulation patterns.

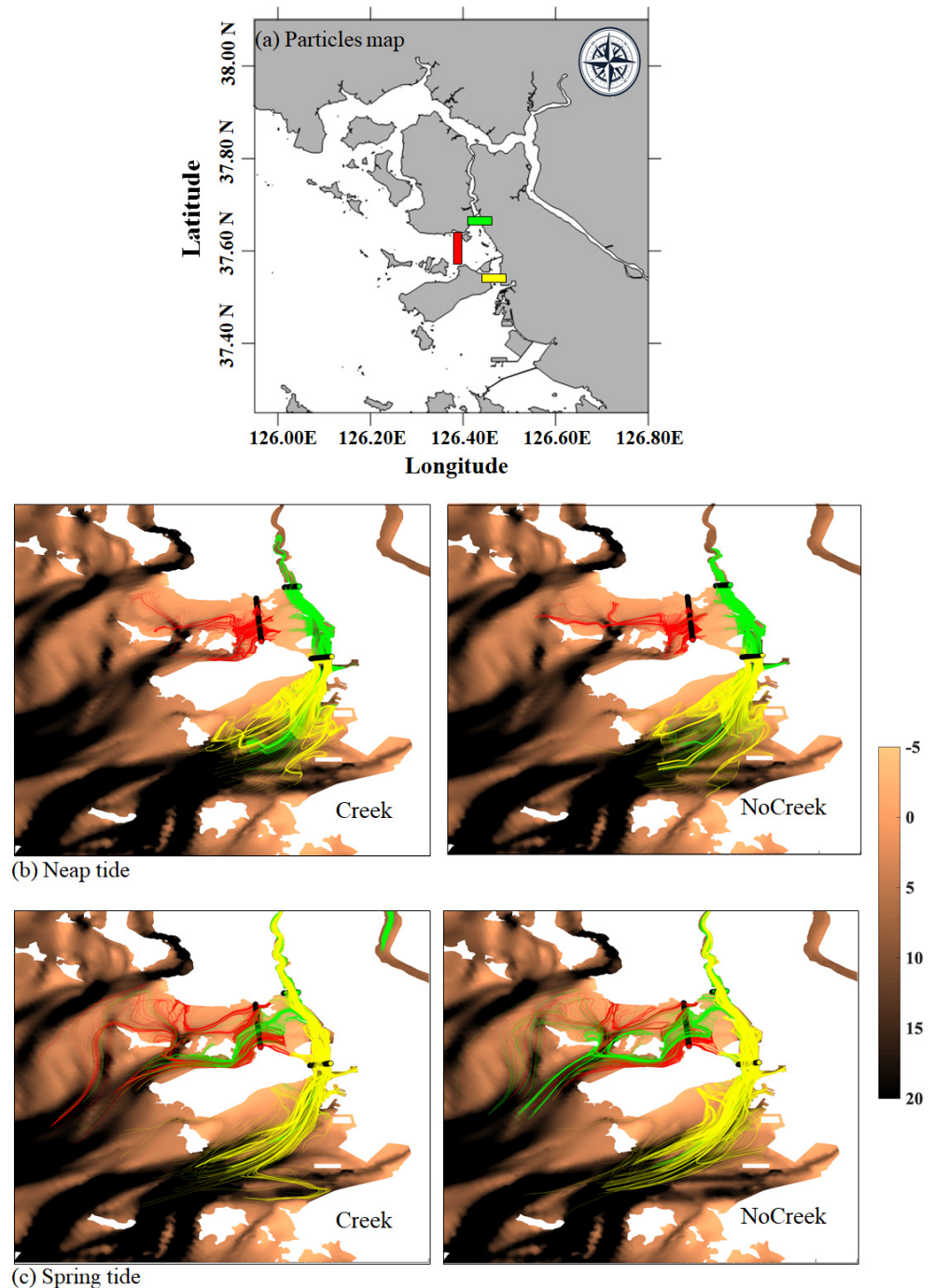
### 3.3. Lagrangian Particle Trajectory

Figure 7 presents the results of a Lagrangian particle trajectory simulation, which was conducted around the tidal creek area by inserting 3000 neutral particles in both the ‘Creek’ and ‘No Creek’ cases. The starting positions of the particles were divided into 3 groups, each represented by 1000 particles in green, red, and yellow colors, corresponding to different areas of the model domain. These particles were evenly distributed across ten sigma layers, making their distribution apparent on the plane.

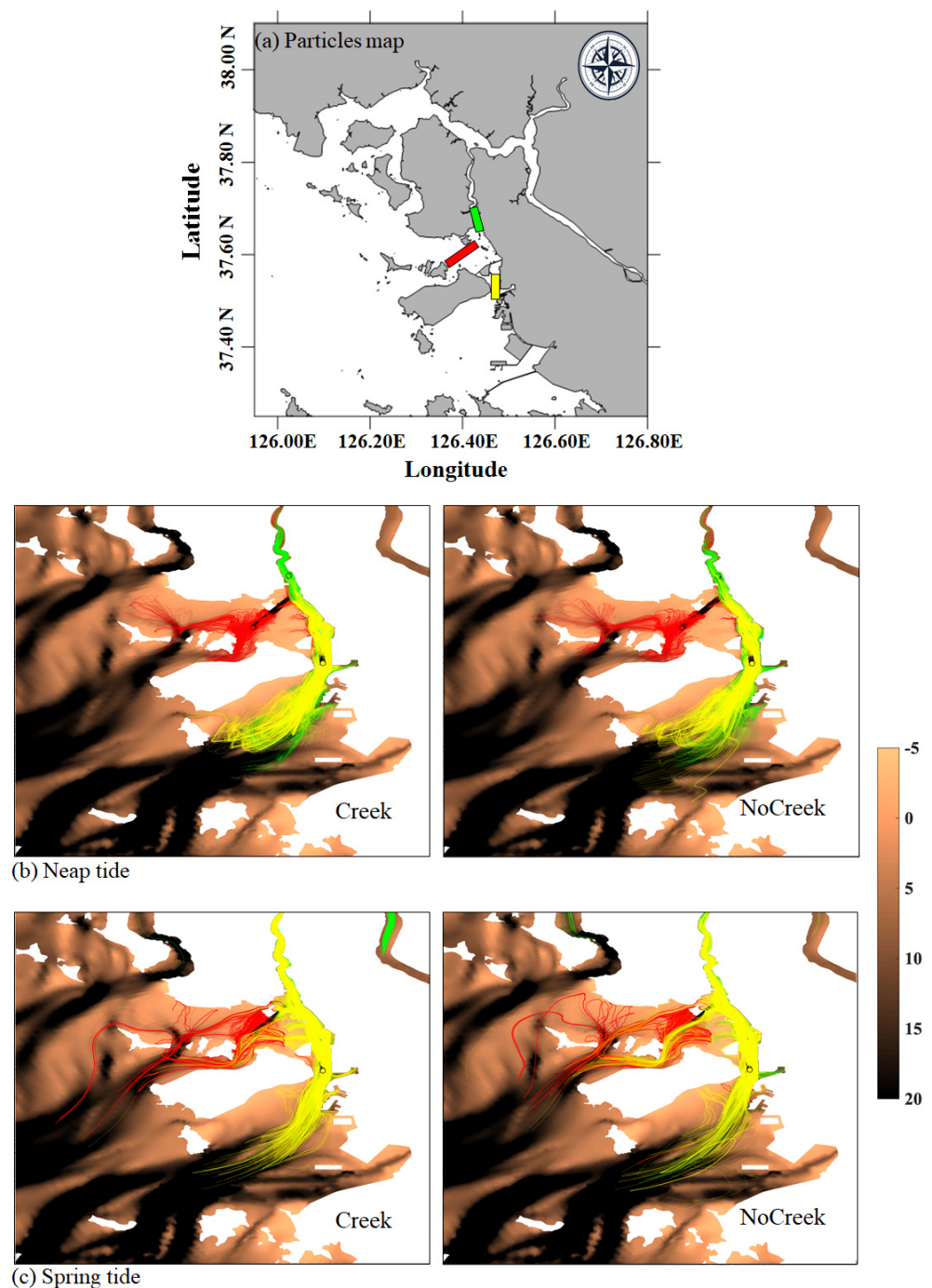
The contours represent bathymetry, where darker shades indicate areas with depths greater than 20 m. Over a two-day exposure period, the trajectories of the particles from the different starting positions reveal intriguing patterns. The red particles, located on the tidal flat, show limited movement, which is attributable solely to tidal currents within the simulation period. In contrast, the green particles, influenced by strong freshwater effects, moved rapidly upstream during the simulation. The yellow particles, starting from the southern part of the tidal channel, exhibited the widest range of movement among the three groups. A comparison between the ‘Creek’ and ‘No Creek’ cases shows notable differences. In the ‘Creek’ case, the particles predominantly move through the tidal flats, likely due to the inclusion of tidal creeks, which act as conduits for the flow. The ‘No Creek’ case, on the other hand, shows that the particles have a tendency to follow the deeper bathymetry contours, resulting in a more constrained and linear dispersion pattern and highlighting the potential limitations in the material circulation.

Figure 8 extends the Lagrangian particle trajectory analysis by modifying the initial placement of the particles to align with the tidal creek, rather than across it, as indicated in Figure 7. This setup provides an insight into the longitudinal transport effects within the ‘Creek’ case. Notably, the green particles in the ‘Creek’ case demonstrate a significant downstream reach, extending to the lower Han River. This characteristic highlights the strong capability of longitudinal flood currents in the ‘Creek’ case to transport particles further downstream, which did not occur in the ‘No Creek’ case. The absence of such downstream transport in the ‘No Creek’ case suggests that the creek’s structure plays a critical role in enabling longitudinal flow and material transport. These results emphasize

the creek's impact on hydrodynamic behavior and its potential implications for sediment transport and estuarine management. The capacity of creeks to affect longitudinal dispersion reinforces the need for detailed representation of these features in hydrodynamic models for estuarine environments.



**Figure 7.** Lagrangian particle trajectories over a two-day period for the 'Creek' and 'No Creek' cases during (b) neap and (c) spring tide, differentiated by color to indicate starting regions within (a) the model domain. Green represents particles influenced by freshwater sources, red indicates particles on the tidal flat, and yellow marks particles originating from the southern part of the tidal channel. The brown contours delineate bathymetry, with darker shades indicating depths exceeding 20 m.



**Figure 8.** Longitudinal Lagrangian particle trajectories for the ‘Creek’ and ‘No Creek’ cases during (b) neap tide and (c) spring tide. (a) Particles were initialized along the tidal creek direction, with the green, red, and yellow colors representing different starting regions.

Figure 9 illustrates the long-term trajectories of the Lagrangian particles over a 40-day period based on their initial positions, as shown in Figure 7. The trajectories reveal significant differences in the maximum range of particle movement between the ‘Creek’ and ‘No Creek’ cases. In the ‘No Creek’ case, the particles exhibit a relatively larger movement range, suggesting that the absence of tidal creeks and flats in the model allows more extensive dispersion. Conversely, in the ‘Creek’ case, particles tend to accumulate within the tidal creeks, though the overall range is not as broad. Notably, the yellow and green particles, initially positioned in the tidal channel, show a distinct spread towards the river mouth in the Creek case.

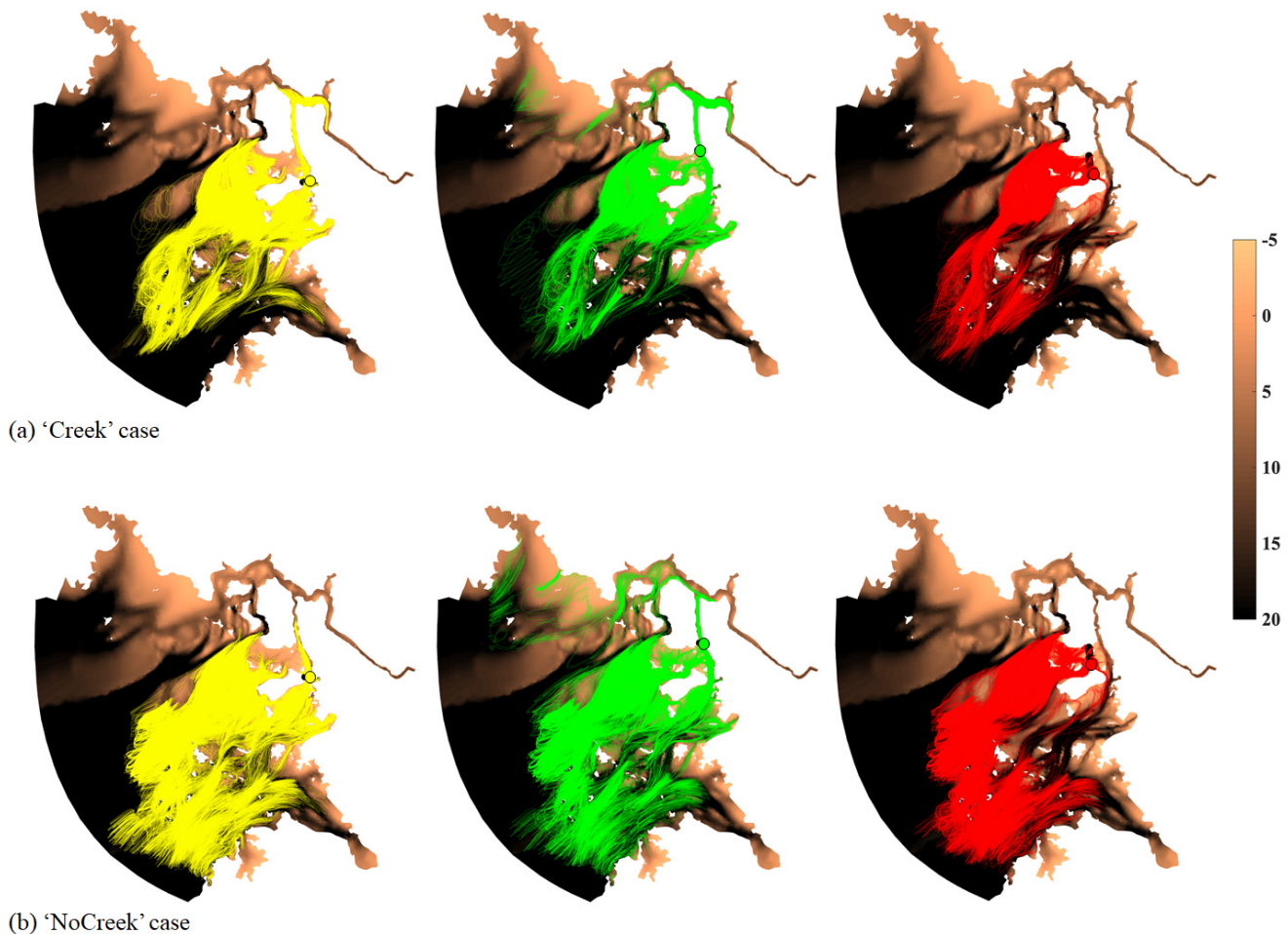


**Figure 9.** Long-term Lagrangian particle trajectories over 40 days in the (a) 'Creek' and (b) 'No Creek' cases. The sequence from left to right represents the spread of particles initially located at the tidal channel (yellow), middle tidal flat (green), and upper tidal flat (red).

Figure 10 refines the analysis of Lagrangian particle movement by isolating representative particles from each group that were initially positioned as shown in Figures 7 and 8, offering a clearer comparison between the 'Creek' and 'No Creek' cases. In the spring tide, particles in the 'Creek' case exhibit more extensive movement, following the direction of the tidal creek. This suggests that the creek's morphology significantly influences particle trajectories as they disperse along the creek path. In contrast, the 'No Creek' case particles quickly drift towards the open sea, implying that the absence of structural constraints allows broader dispersion. During neap tides, the 'No Creek' case shows the particles moving faster, likely driven by the prevailing ebb flow. This faster movement could be indicative of lower shear stress, which is a consequence of not considering the tidal creek's influence, which typically acts as a boundary that modulates flow and sediment transport. Overall, Figure 10 demonstrates that the presence of tidal creeks has a profound impact on particle movement, especially in terms of directionality and the extent of the transport.

Building on the initial analysis, the selection process for representative particles from Figures 7–9 focused on capturing distinct trajectories to elucidate clear movement patterns. While overall directionality and dispersion can be inferred from long-term or short-term observations, pinpointing precise pathways proves challenging without considering nonlinear dynamics, especially in tidal flats. Averaging the positions only based on location risks oversimplifying these dynamics, potentially erasing the nonlinear effects observed in tidal areas. Therefore, representative particles were chosen based on trajectory concentration, favoring a qualitative over a numerical approach, given the minimal depth variation across the water column in these selected areas. Central positions were preferred to avoid particles

adhering to the coastline; such particles often struggle to detach due to the shallow depths. This methodological choice acknowledges the potential for increased error when averaging particle positions discretely or through ensemble means. By iterating this selection process and focusing on trajectory density, we meticulously identified representative particles for each group, ensuring a comprehensive portrayal of particle movement that retains the inherent complexity and variability within the estuarine system.

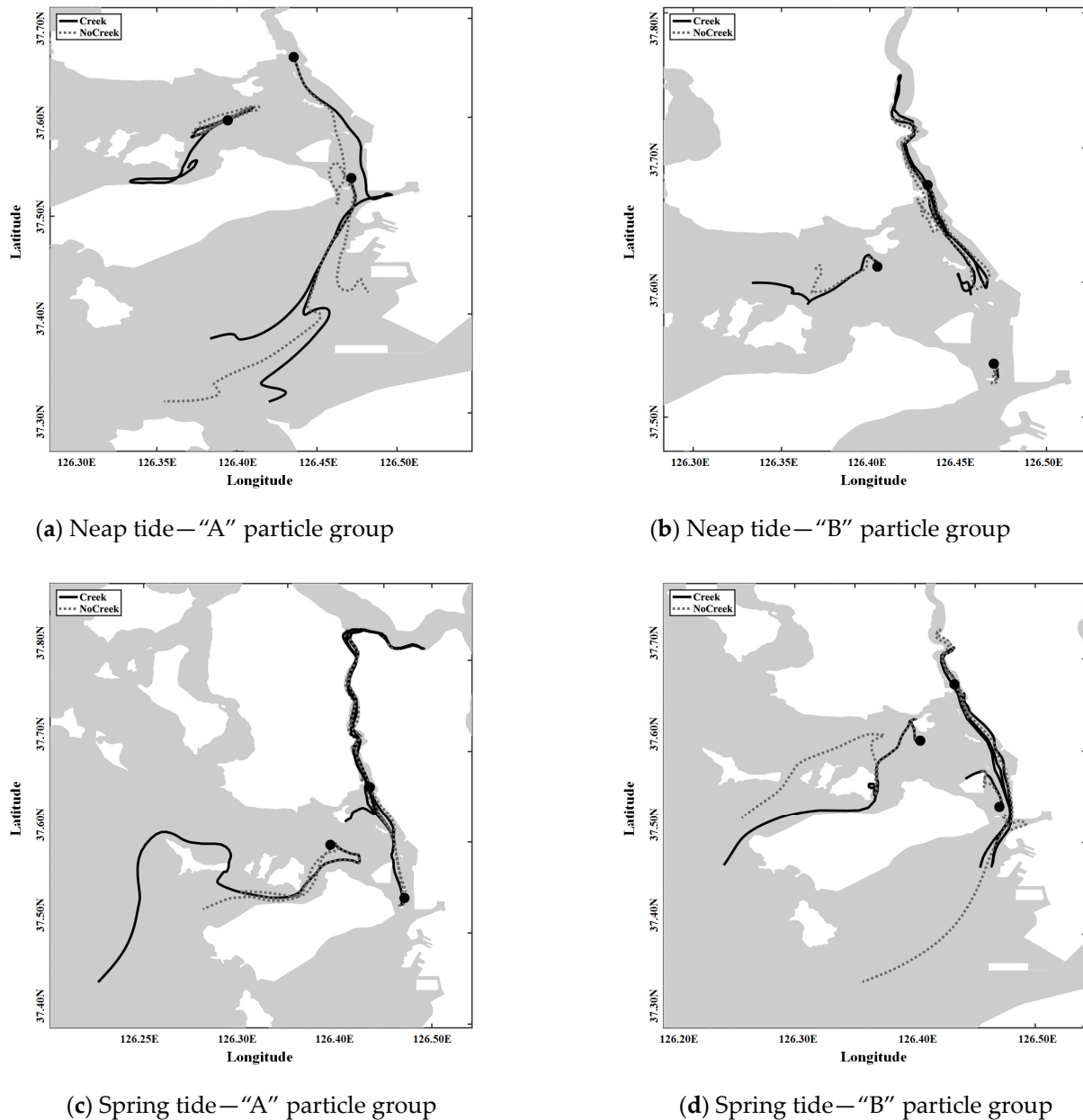


**Figure 10.** Trajectories of representative particles from group ‘A’ originating from the initial positions used in Figure 7 (panels (a,c)) and group ‘B’ from Figure 8 (panels (b,d)), shown during neap and spring tides. The solid lines track particle paths within the Creek case, while the dotted lines show movements in the No Creek case, demonstrating the contrasting dispersion influenced by the presence or absence of tidal creek structures.

#### 4. Discussion

This study significantly contributes to the understanding of estuarine hydrodynamics by examining the interplay between the geomorphological features and hydrodynamic processes within macro-tidal flat environments. By integrating detailed residual current

analyses and employing unstructured grids, this research offers a nuanced approach to the modeling of estuarine systems, which is crucial for predicting contaminant transport accurately. The 'Creek' case demonstrates the profound influence of tidal creeks on estuarine hydrodynamics, enhancing particle retention and potentially boosting nutrient cycling within these environments. This highlights the necessity of incorporating the complex interactions of Stokes drift and Eulerian and Lagrangian residuals in coastal models, especially in macro-tidal environments where tidal forces play a significant role in shaping the sediment and nutrient dynamics. Comparative studies from different estuaries, such as the Yellow Sea [14], highlight the impact of environmental factors, like solar radiation, wind forcing, river discharge, tides, and water exchange, on coastal morphology and oceanographic conditions. The Yellow Sea's macro-tidal nature, with significant seasonal variability influenced by the Asian monsoon system, shares similarities with our study area, emphasizing the importance of considering such dynamic environmental conditions in estuarine modeling. Furthermore, the deployment strategies for monitoring systems in estuaries, as discussed in reference [14], underscore the critical need to strategically monitor location selection to capture changes in water quality and pollutants effectively. Based on spatial and temporal optimizations, these strategies align with our approach of using advanced modeling techniques to understand and predict the complexities of estuarine environments. Our study's findings, set against the backdrop of these comparative analyses, highlight the unique aspects of our research area and the importance of accurately representing tidal channels in hydrodynamic models. The enhanced capacity for material transport observed in the 'Creek' case during spring tides underscores the critical role of tidal creeks in estuarine systems, necessitating accurate tidal channel representation for reliable transport predictions and a deeper understanding of coastal estuarine transport mechanisms. By drawing insights from various studies [14], our research contributes to a broader understanding of estuarine dynamics and the development of more effective environmental management and conservation strategies tailored to the macro-tidal flat environments' specific needs and characteristics.

The significance of salinity stratification in estuarine systems, particularly during neap tides, is a pivotal factor influencing vertical mixing and the distribution of biological and chemical components. This study's 'Creek' case highlights how pronounced stratification could shape the vertical dispersal of larvae, nutrients, and pollutants, which significantly impact the estuarine ecosystem and sediment dynamics. Such stratification effects on species distribution, behavior, and sedimentary processes underscore the need for models that intricately integrate geomorphological features and their hydrodynamic influences for precise material flux predictions in estuaries. Drawing parallels from field observations in the Geum River estuary [15], where artificial gate operations modulate stratification and tidal amplitudes drive mixing, our study underscores the complexity of the stratification processes influenced by natural and anthropogenic factors. As with the dynamics observed in the Geum River, our study's 'Creek' case presents a scenario where tidal creeks significantly modulate the estuarine stratification, thereby affecting the estuarine dynamics and ecological balance. The exploration of advection, straining, and vertical mixing in estuarine stratification [15] resonates with our findings and emphasizes these processes' critical roles in shaping the estuarine water body's vertical density structure. The FVCOM application in the Seomjin River estuary highlights how straining and mixing govern the flow and stratification structures, which are akin to the stratification dynamics observed in our 'Creek' case. This parallel draws attention to the importance of considering the balance between mixing and straining in determining the stratification type in estuarine channels and further validates the nuanced approach of our study in capturing these intricate interactions. Moreover, the study on the impact of artificially discharged freshwater in a Korean estuary [15] provides insights into how discharged freshwater cyclically forms stratified layers during ebb tides and mixes during flood tides, aligning with the stratification and mixing patterns observed in our 'Creek' case. This cyclic pattern, characterized by the gradient Richardson number, offers a quantitative framework to assess



the interplay between stratification and mixing in estuarine environments, reinforcing the necessity of incorporating such dynamic processes in estuarine modeling for effective environmental management and strategy formulation. The integration of the insights from these studies [15] with our research findings elucidates the multifaceted nature of estuarine stratification and its implications for material transport and ecosystem dynamics. The comparative analysis not only highlights the unique aspects of our study area but also emphasizes the overarching need for comprehensive hydrodynamic models that reflect the intricate interplay of geomorphological features and hydrodynamic processes in estuarine systems and ensure accurate predictions and effective management strategies in these dynamic and complex environments.

By integrating LPT models, this study advances the comprehension of particle dynamics by delving into the complexities of contaminant transport within macro-tidal flats. The influence of tidal and freshwater forces on salt intrusion and suspended sediment dynamics is assessed, echoing the necessity for high-resolution modeling, as demonstrated in the Changjiang River study [16]. This underscores the critical need to capture complex nonlinear interactions and to integrate high grid resolution for accurate hydrodynamic behavior modeling in estuarine systems. Our findings reveal distinct particle movements in the 'Creek' and 'No Creek' cases, emphasizing the geomorphological impact on coastal circulation. This is similar to the observations in the southeastern North Sea, where human-made structures affected sediment dynamics [17]. The study suggests that tidal creeks act as natural modulators of flow and sediment deposition, significantly impacting estuarine geomorphology and habitats [18]. This is further supported by the alignment of our study with the investigations into Lake Erie's harmful algal blooms; these investigations highlight the utility of both Lagrangian and Eulerian models in forecasting ecosystem responses and the potential for hybrid approaches that can enhance future models [19]. The research integrates advanced modeling techniques and insights from various studies, highlighting the significant role of geomorphological features and their interaction with hydrodynamic processes [20–22]. The analysis of 'Creek' and 'No Creek' cases provides new insights into the protective role of tidal creeks in material transport within estuarine systems. This novel approach enhances our understanding of estuarine dynamics and aids in the development of effective environmental management and conservation strategies. The FVCOM framework used in our research corresponds with the latest advancements in coastal modeling, like the FESOM-C application in the southeastern North Sea [20]. The unstructured grid design of the FVCOM is crucial for simulating complex estuarine dynamics and offers refined meshing to capture small-scale processes effectively. Adjusting mesh resolution according to specific geographical and process requirements, validated against high-resolution observational data [20], highlights the efficacy of such models in capturing the environmental intricacies of estuarine systems. While high-resolution wave coupling models provide precision in short-term forecasting through the Navier–Stokes equations [23,24], incorporating them into three-dimensional flow-based LPT studies presents a challenge. Our methodology, which harmonizes Lagrangian and Eulerian perspectives, offers a promising avenue for the enhancement of the predictive accuracy and depth of analysis for contamination distribution studies in estuarine contexts. This integration of modeling techniques affords a comprehensive understanding of contaminant dynamics, informed by the pollutants' final positions and the broader hydrodynamic interactions within estuarine systems.

The presence of tidal creeks significantly influences particle dispersion and material transport, implying a more intricate and dispersed transport mechanism provided by the additional pathways within the 'Creek' case. This complexity highlights the need for hydrodynamic models to accurately account for such features to make precise material transport predictions in estuarine environments. Suppose the tracked particles are representative of pollutants. In that case, the 'Creek' case demonstrates a swift dispersion to downstream river areas, underscoring the pivotal role of tidal channels in substance transport and distribution. This dynamic is crucial for environmental management, emphasizing the necessity for targeted strategies to mitigate pollution risks in riverine and coastal ecosystems [25–27].

The results of this study provide valuable insights for environmental management and policy making, particularly in the context of mitigating pollution risks in estuarine and coastal areas.

## 5. Conclusions

This study provides crucial insights into estuarine hydrodynamics and particularly emphasizes the role of tidal creeks in contaminant transport. The study unravels the intricate interplay between the physical structures and flow patterns that are crucial in determining the dispersion and retention of contaminants.

1. This research highlights the importance of including the geometrical complexities of tidal creeks in contaminant transport models. The ‘Creek’ case demonstrated how these features substantially influence flow patterns, leading to enhanced retention of contaminants within the estuarine system. This enhanced retention can significantly affect the bioavailability and degradation rates of contaminants due to changes in exposure durations.
2. The distinct dispersion behaviors in the ‘No Creek’ case suggest a risk related to the underestimation of contaminant retention within the estuary and the overestimation of their dispersion to coastal waters when such structural complexities are not considered. This insight is vital for precise contaminant budget assessments and the development of effective mitigation strategies in estuarine environments.
3. The variation in the stratification during neap tides leads to the role of vertical mixing in contaminant distribution; this is an aspect which is crucial for the understanding of the vertical contaminant concentration profiles and their potential impacts across different trophic levels within the estuarine food web.

In conclusion, this study highlights the complex relationship between estuarine morphology and contaminant transport processes. Accurately representing tidal creek dynamics is crucial for developing predictive models for managing the risks associated with contaminant spread in estuarine and coastal ecosystems. Future research should focus on observational network design techniques, as demonstrated in references [28–30], with operational forecasting systems and LPT techniques. This integration aims to develop an optimized observational network for automatic monitoring instruments, enhancing the precision and efficiency of data collection in estuarine environments. Additionally, it is imperative to continue refining these models by incorporating detailed morphological data, which will significantly improve the accuracy of long-term contaminant behavior predictions. Such advancements are crucial for the devising of effective environmental management strategies and policies to ensure the sustainability and health of estuarine ecosystems.

## Appendix A

Appendix Figure A1 is a necessary supplementary validation of this study’s surface residual currents that prominently influence particle tracking. While this paper details current, salinity, turbulent diffusion coefficients, bottom roughness, and various parameters, including resolution, element, and node size, it is challenging to encompass all these factors comprehensively. Thus, residual current validation is included in the appendix to discern the distinct effects of tidal channel considerations when viewed from a Lagrangian perspective, which is mainly based on residual components. A notable feature in Lines 1 and 2 is the Creek case’s resemblance to observed Lagrangian residual transport rates. Moreover, while the Eulerian residual transport rates show a slight variation between the two experiments, the Stokes drift presents an intriguing contrast, with residuals indicating opposite directions. This appendix underscores the nuanced hydrodynamic effects captured by considering tidal channels and offers an in-depth comparative assessment of the modeled and observed residual currents, enriching the study’s validation process.

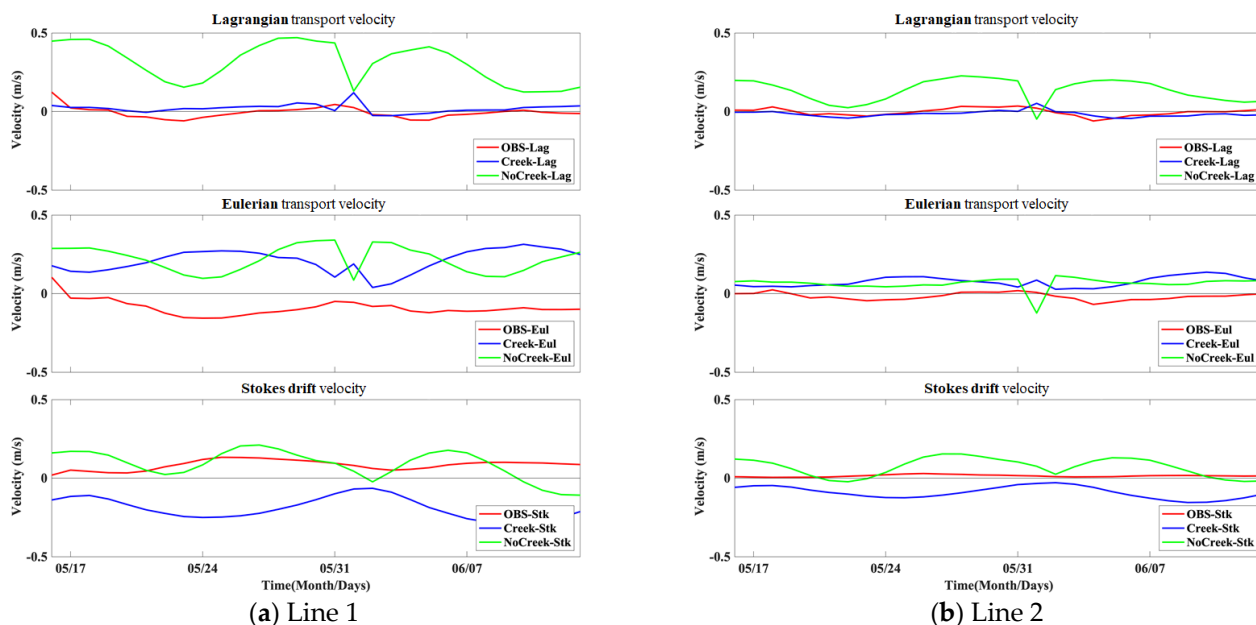


**Figure A1.** Comparative analysis of surface residual currents between ‘Creek’ and ‘No Creek’ cases. This figure illustrates a side-by-side comparison of the surface residual currents for the ‘Creek’ and ‘No Creek’ scenarios within the study’s estuarine environment. The top panel demonstrates the Lagrangian residual transport velocities, indicating the alignment of the ‘Creek’ case with observed data (OBS) and highlighting the model’s accuracy in simulating surface currents under the influence of tidal creeks. The middle panel depicts Eulerian transport velocities, indicating minimal discrepancy between the two experimental setups, reflecting the models’ capability to capture the estuary’s general flow patterns. The bottom panel presents the Stokes drift velocities, highlighting a pronounced difference in the directionality of the residuals, evidencing the significant impact of creek morphology on surface current characteristics. This appendix figure supplements the main text’s discussion, providing an extended validation of the models’ hydrodynamic simulations, specifically focusing on the surface layer that predominantly governs particle trajectories in the estuarine system.

**Author Contributions:** B.-H.G. designed the study, wrote the manuscript, and coordinated the writing team. N.-H.K. contributed to the introduction and conclusion from the perspective of coastal oceanography. J.-I.K. presented research cases related to marine debris and contributed to the differentiation of this study. S.-B.W. collected observational data for numerical model validation and contributed to residual volume transport analysis. S.-H.P. contributed substantially to the methodology of particle tracking, ensuring the stability of the model simulations. All authors have read and agreed to the published version of the manuscript.

**Funding:** This research was supported by Korea Institute of Marine Science & Technology Promotion (KIMST) funded by the Ministry of Oceans and Fisheries, Korea (20180447, Improvements of ocean prediction accuracy using numerical modeling and artificial intelligence technology). This research was also supported by an in-house grant from KIOST (PEA0231, research on prediction techniques to reduce damage from marine disasters).

**Data Availability Statement:** The data used in this study are available on request from the first author.

**Conflicts of Interest:** The authors declare no conflicts of interest.

## References

1. Aubrey, D.G.; Speer, P.E. A Study of Non-Linear Tidal Propagation in Shallow Inlet Estuarine Systems Part I: Observations. *Estuar. Coast. Shelf Sci.* **1985**, *21*, 185–205. [\[CrossRef\]](#)
2. Speer, P.E.; Aubrey, D.G. A Study of Non-Linear Tidal Propagation in Shallow Inlet Estuarine Systems Part II: Theory. *Estuar. Coast. Shelf Sci.* **1985**, *21*, 207–224. [\[CrossRef\]](#)
3. Murty, T.S. Nonlinear Tidal Distortion in Shallow Well-Mixed Estuaries. *Estuar. Coast. Shelf Sci.* **1990**, *30*, 321–322. [\[CrossRef\]](#)
4. Lanzoni, S.; Seminara, G. On tide propagation in convergent estuaries. *J. Geophys. Res.-Ocean.* **1998**, *103*, 30793–30812. [\[CrossRef\]](#)

5. Blanton, J.O.; Lin, G.Q.; Elston, S.A. Tidal current asymmetry in shallow estuaries and tidal creeks. *Cont. Shelf Res.* **2002**, *22*, 1731–1743. [[CrossRef](#)]
6. Kim, C.S.; Lim, H.S.; Kim, J.; Kim, S.; Park, K.S.; Jung, K.T. Estimation of Tidal Residual Flow and Its Variability in Kyunggi Bay of Korea. *J. Korean Soc. Mar. Environ. Energy* **2010**, *22*, 353–360.
7. Yoon, B.I.; Woo, S.-B. Study on Relationship Between Geographical Convergence and Bottom Friction at the Major Waterways in Han River Estuary using the Tidal Wave Propagation Characteristics. *J. Korean Soc. Coast. Ocean Eng.* **2011**, *23*, 383–392. [[CrossRef](#)]
8. Park, K.; Oh, J.H.; Kim, H.S.; Im, H.H. Case study: Mass transport mechanism in Kyunggi Bay around Han River Mouth, Korea. *J. Hydraul. Eng.-ASCE* **2002**, *128*, 257–267. [[CrossRef](#)]
9. Kang, J.W.; Park, S.J.; Kim, Y.S.; So, J.K. Tidal Flat Simulation Characteristics of the Hydrodynamic Models. *J. Korean Soc. Coast. Ocean. Eng.* **2009**, *21*, 357–370.
10. Chen, C.S.; Liu, H.D.; Beardsley, R.C. An unstructured grid, finite-volume, three-dimensional, primitive equations ocean model: Application to coastal ocean and estuaries. *J. Atmos. Ocean. Technol.* **2003**, *20*, 159–186. [[CrossRef](#)]
11. Lee, D.H.; Yoon, B.I.; Woo, S.-B. The Cross-Sectional Characteristic and Spring-Neap Variation of Residual Current and Net Volume Transport at the Yeomha Channel. *J. Korean Soc. Coast. Ocean. Eng.* **2017**, *29*, 217–227. [[CrossRef](#)]
12. Foreman, M.G.G.; Henry, R.F. The Harmonic-Analysis of Tidal Model Time-Series. *Adv. Water Resour.* **1989**, *12*, 109–120. [[CrossRef](#)]
13. Sylaios, G.; Boxall, S.R. Residual currents and flux estimates in a partially-mixed estuary. *Estuar. Coast. Shelf Sci.* **1998**, *46*, 671–682. [[CrossRef](#)]
14. Hwang, J.H.; Van, S.P.; Choi, B.-J.; Chang, Y.S.; Kim, Y.H. The physical processes in the Yellow Sea. *Ocean. Coast. Manag.* **2014**, *102*, 449–457. [[CrossRef](#)]
15. Hwang, J.H.; Jang, D.; Kim, Y.H. Stratification and salt-wedge in the Seomjin river estuary under the idealized tidal influence. *Ocean. Sci. J.* **2017**, *52*, 469–487. [[CrossRef](#)]
16. Xue, P.; Chen, C.; Ding, P.; Beardsley, R.C.; Lin, H.; Ge, J.; Kong, Y. Saltwater intrusion into the Changjiang River: A model-guided mechanism study. *J. Geophys. Res. Ocean.* **2009**, *114*, C02006. [[CrossRef](#)]
17. Hache, I.; Niehüser, S.; Karius, V.; Arns, A.; von Eynatten, H. Assessing sediment accumulation at inundated anthropogenic marshland in the southeastern North Sea: Using particle tracking on modified coastal protection structures. *Ocean Coast. Manag.* **2021**, *208*, 105631. [[CrossRef](#)]
18. Zhao, E.-J.; Mu, L.; Qu, K.; Shi, B.; Ren, X.-Y.; Jiang, C.-B. Numerical investigation of pollution transport and environmental improvement measures in a tidal bay based on a Lagrangian particle-tracking model. *Water Sci. Eng.* **2018**, *11*, 23–38. [[CrossRef](#)]
19. Zhou, X.; Rowe, M.; Liu, Q.; Xue, P. Comparison of Eulerian and Lagrangian transport models for harmful algal bloom forecasts in Lake Erie. *Environ. Model. Softw.* **2023**, *162*, 105641. [[CrossRef](#)]
20. Kuznetsov, I.; Androsov, A.; Fofonova, V.; Danilov, S.; Rakowsky, N.; Harig, S.; Wiltshire, K.H. Evaluation and Application of Newly Designed Finite Volume Coastal Model FESOM-C, Effect of Variable Resolution in the Southeastern North Sea. *Water* **2020**, *12*, 1412. [[CrossRef](#)]
21. Guo, Q.; Zhang, Y.; Zhou, Z.; Hu, Z. Transport of Contamination under the Influence of Sea Level Rise in Coastal Heterogeneous Aquifer. *Sustainability* **2020**, *12*, 9838. [[CrossRef](#)]
22. Zhang, Q.; Volker, R.E.; Lockington, D.A. Experimental investigation of contaminant transport in coastal groundwater. *Adv. Environ. Res.* **2002**, *6*, 229–237. [[CrossRef](#)]
23. Jones, J.E.; Davies, A.M. An intercomparison between finite difference and finite element (TELEMAC) approaches to modelling west coast of Britain tides. *Ocean Dyn.* **2005**, *55*, 178–198. [[CrossRef](#)]
24. Dietrich, J.C.; Tanaka, S.; Westerink, J.J.; Dawson, C.N.; Luettich, R.A.; Zijlema, M.; Holthuijsen, L.H.; Smith, J.M.; Westerink, L.G.; Westerink, H.J. Performance of the Unstructured-Mesh, SWAN+ADCIRC Model in Computing Hurricane Waves and Surge. *J. Sci. Comput.* **2011**, *52*, 468–497. [[CrossRef](#)]
25. Xue, P.; Schwab, D.; Zhou, X.; Huang, C.; Kibler, R.; Ye, X. A Hybrid Lagrangian–Eulerian Particle Model for Ecosystem Simulation. *J. Mar. Sci. Eng.* **2018**, *6*, 109. [[CrossRef](#)]
26. Pilechi, A.; Mohammadian, A.; Murphy, E. A numerical framework for modeling fate and transport of microplastics in inland and coastal waters. *Mar. Pollut. Bull.* **2022**, *184*, 114119. [[CrossRef](#)] [[PubMed](#)]
27. Kim, D.H.; Hwang, J.H.; Jeong, J.; Hong, Y.; Lee, M. Comprehensive modeling from watersheds to a bay and its validation with radar, drifters, and MVP methods. *Reg. Stud. Mar. Sci.* **2023**, *68*, 103262. [[CrossRef](#)]
28. Oke, P.R.; Brassington, G.B.; Griffin, D.A.; Schiller, A. The Bluelink ocean data assimilation system (BODAS). *Ocean Model.* **2008**, *21*, 46–70. [[CrossRef](#)]
29. Kim, N.-H.; Baek, D.; Kwon, J.-I.; Choi, J.-Y.; Heo, K.-Y. Strategy for additional buoy array installation in operational buoy-observation network in Korea. *Ocean Eng.* **2022**, *266*, 112746. [[CrossRef](#)]
30. Oliveira, A.; Fortunato, A.B.; Rogeiro, J.; Teixeira, J.; Azevedo, A.; Lavaud, L.; Bertin, X.; Gomes, J.; David, M.; Pina, J.; et al. OPENCoastS: An open-access service for the automatic generation of coastal forecast systems. *Environ. Model. Softw.* **2020**, *124*, 104585. [[CrossRef](#)]

**Disclaimer/Publisher’s Note:** The statements, opinions and data contained in all publications are solely those of the individual author(s) and contributor(s) and not of MDPI and/or the editor(s). MDPI and/or the editor(s) disclaim responsibility for any injury to people or property resulting from any ideas, methods, instructions or products referred to in the content.